Stability Analysis of a DiffServ Network Having Two-Level Coloring at the Network Edge and Preferential Dropping at the Core

Y. Cui, Y. Chait, and C.V. Hollot

Abstract

This paper presents a local stability result for Differentiated Services (DiffServ) networks with heterogeneous TCP flows consisting of two-level edge coloring using a token bucket, and preferentially-dropping core router. Coloring is accomplished using a recently proposed edge mechanism to adaptively tune the token-bucket rate. The result is stated for sources under TCP-Reno congestion control algorithm. Stability analysis of several DiffServ networks that were tested using ns simulations is described.

I. Introduction

The Internet was originally designed as, and by-and-large is still a framework for providing best-effort services. Traffic is processed as quickly as possible but without any guarantee of timeliness of actual delivery. In recent years, new applications have sprung which require some form of quality of service (QoS) guarantee from the network. The Internet Engineering Task Force (IETF) has proposed service models and mechanisms to meet the demand for QoS. Notably among them are the Integrated Services/Resource Reservation Protocol (RSVP) model, the Differentiated Services (DiffServ) model, multi-protocol label switching (MPLS) and traffic engineering. Here we focus on DiffServ which provides a scalable solution since the amount of state information is proportional to the number of contract-paying sources rather than the total number of flows. Two per-hop behaviors (PHBs) have been standardized by IETF, expedited forwarding (EF) [1] and assured forwarding (AF) [2]. The former is intended to support low delay applications while the latter is intended to provide throughput differentiation among clients according to negotiated profiles.

Our DiffServ network is based on the AF PHB. There are several traffic management and packet marking mechanisms proposed for AF DiffServ, all sharing the following basic idea. Coloring edges employ token buckets; packets that originally conform to bucket parameters (a function of a negotiated profile) are colored green and excess packets remain unmarked (colored red). Core routers give preference to green packets. In the presence of congestion, red packets are more likely to be dropped (or have their congestion notification bit set in the presence of the Explicit Congestion Notification (ECN)) [3]. Several studies have shown that the throughput attained by a customer is affected not only by the edge marker but also by the presence of other customer flows and propagation delays [4]-[6]. This is because the predominance of traffic is carried by TCP (of various variants) whose congestion avoidance mechanism reacts in a complex manner with its environment. In [7], an *Active Rate Management* (ARM) mechanism was introduced to overcome this limitation. The basic idea is that the edges maintain ARMs which are responsible for adaptively setting token bucket parameters in order to achieve minimum throughputs in the face of changing network parameters. ns simulations in [7] demonstrated that when combined with two-level PI-AQM [8] at differentiating cores, this ARM mechanism is able to maintain minimum throughputs at or above target rates and is able to respond in a timely manner to fluctuations in traffic characteristics.

In this paper, using robust stability formulation, we analyze the effect of introducing this ARM mechanism into a stable TCP-Reno network employing PI AQM at the core. Our local stability conditions highlight the interplay between AQM and ARM and can be recast as design rules for AQM and ARM controllers. This defines the contribution of our work. The remainder of the paper is organized as follows. In Section 2 we describe a fluid model for the dynamics of the network. In Section 3 we develop linearized models for control design and analysis (details are given in Appendix A), then describe general types of AQM and ARM controllers for this problem.

This work is supported by the National Science Foundation under Grant ANI-0125979.

Y. Cui is with the MIE Department, University of Massachusetts, Amherst, MA 01003; ycui@ecs.umass.edu.
Y. Chait is with the MIE Department, University of Massachusetts, Amherst, MA 01003; chait@ecs.umass.edu.
C.V. Hollot is with the ECE Department, University of Massachusetts, Amherst, MA 01003; hollot@ecs.umass.edu.

In Section 4, we state our main theorem that proves existence of stabilizing ARM and AQM controllers. Stability analysis of an over-provisioned and under-provisioned DiffServ networks tested in ns is presented in section 5. We note our parallel work in [9] which quantifies behavior of bucket-rate adaptation and preferential dropping that guarantees minimum throughput to users under general congestion control sources that include TCP-Reno and proportionally-fair schemes.

II. The DiffServ Network Model

In this section, we introduce a fluid flow model for the dynamics of a DiffServ network consisting of heterogeneous TCP-controlled sources[1], AQM-controlled core router and coloring edge routers using token buckets. Our starting point is [10] which presented a fluid flow approach for modelling TCP flows and AQM routers and the extension in [7] to account for two-color marking at the network edge and multi-level AQM at the core. The network has n classes of aggregate heterogeneous flows, termed *sources*, each consisting of η_i identical TCP flows. Without loss of generality, we assume that each such source is served by a separate edge that includes a token bucket with rate A_i and size $b_i >> 1$. The sources feed into a core router with link capacity c and queue length denoted by $q(t)$. A generic TCP flow in the i-th source is characterized by its window size $W_i(t)$ given by

$$\frac{dW_i(t)}{dt} = \frac{1 - p_i(t - \tau_i(t))}{\tau_i(t)} - \frac{W_i(t)W_i(t - \tau_i(t))}{2\tau_i(t - \tau_i(t))} p_i(t - \tau_i(t)), \tag{1}$$

where $p_i(t)$ denotes the probability that ECN bit is set for the i-th source[2]. The average round-trip time $\tau_i(t)$ is

$$\tau_i(t) \stackrel{\triangle}{=} T_{pi} + \frac{q(t)}{c}, \tag{2}$$

where T_{pi} is the i-th source propagation delay. The source instantaneous send rate x_i is described by

$$x_i = \frac{\eta_i W_i(t)}{\tau_i(t)}. \tag{3}$$

The dynamics of the core's buffer is described by

$$\frac{dq(t)}{dt} = -cI_{q>0} + \sum_{i=1}^{n} x_i, \tag{4}$$

where $I_{q>0}$ is the indicator function.

Finally, we model the coloring process at an edge and multi-level AQM action at the core. To model coloring, let $f_{gi}(t)$ denote the fraction of fluid from i-th source marked green (i.e., flow within target rate) where

$$f_{gi}(t) = \min\left\{1, \frac{A_i(t)}{x_i(t)}\right\},$$

and $1 - f_{gi}(t)$ denotes the red fraction of flow (exceeding target rate). At the core, $p_g(t)$ and $p_r(t)$ denote the probabilities that ECN marks are generated for the green and red fluids, respectively[3]. According to [14], we have $0 \leq p_g(t) < p_r(t) \leq 1$. The i-th source's loss probability $p_i(t)$ is then related to the green and red marks by

$$p_i(t) = f_{gi}(t)p_g(t) + (1 - f_{gi}(t))p_r(t).$$

Next, in preparation for stability analysis of the network, we derive a linearized model about equilibrium.

III. Linearized Network Model

In this section, we linearize the network model (1)-(5) about equilibrium, then form control block diagram suited for stability analysis. We follow with the token bucket controllers and AQMs which complete description of the closed-loop system.

[1]Throughout this paper the term TCP-controlled sources refers to AIMD-like sources (e.g. TCP-Reno and TCP-SACK).

[2]The $1 - p_i$ term in the additive part does not appear in [7], but has appeared since in several publications, e.g., [11].

[3]More precisely, marks are embedded in the fluid as a time varying Poisson process, and the product of p_g and p_r with the green and red fluid throughputs, respectively, determines the intensity of this Poisson process.

A. Open-Loop Model

We begin by writing the model explicitly in terms of the bucket rates A_i:

$$\begin{aligned}
\dot{q} &= -cI_{q>0} + \sum_{i=1}^{n} \frac{\eta_i W_i(t)}{\tau_i(t)} \\
&\triangleq f(q, W_i, p_g, p_r, A_i); \\
\dot{W}_i &= \frac{1 - p_i(t-\tau_i(t))}{\tau_i(t)} - \frac{W_i(t) W_i(t-\tau_i(t))}{2\tau_i(t-\tau_i(t))} p_i(t-\tau_i(t)) \\
&\triangleq g_i(q, W_i, p_g, p_r, A_i)
\end{aligned}$$

where

$$p_i(t-\tau_i(t)) = \left(\frac{A_i}{x_i(t)} p_g(t-\tau_i(t)) + \ (1 - \frac{A_i}{x_i(t)}) p_r(t-\tau_i(t)) \right).$$

Let the equilibrium state be denoted by $(\hat{q}, \hat{W}_i, \hat{p_g}, \hat{p_r}, \hat{A}_i)$ and denote perturbations about equilibrium by

$$\begin{aligned}
\delta q &\triangleq q(t) - \hat{q} \\
\delta W_i &\triangleq W_i(t) - \hat{W}_i \\
\delta p_g &\triangleq p_g(t) - \hat{p_g} \\
\delta p_r &\triangleq p_r(t) - \hat{p_r} \\
\delta A_i &\triangleq A_i(t) - \hat{A}_i.
\end{aligned}$$

The linearized open-loop network model can be shown to be (see Appendix A for details)

$$\delta W_i(s) = \frac{\frac{\partial g_i}{\partial A_i}}{s - \frac{\partial g_i}{\partial W_i}} \delta A_i(s) + \frac{\frac{\partial g_i}{\partial p_g}}{s - \frac{\partial g_i}{\partial W_i}} e^{-s\tau_i} \delta p_g(s) + \frac{\frac{\partial g_i}{\partial p_r}}{s - \frac{\partial g_i}{\partial W_i}} e^{-s\tau_i} \delta p_r(s) \tag{5}$$

$$\delta q(s) = \sum_{i=1}^{n} \frac{\frac{\partial f}{\partial W_i}}{s - \frac{\partial f}{\partial q}} \delta W_i(s). \tag{6}$$

In Appendix B it is shown that at equilibrium, either $\delta p_r(s)$ or $\delta p_g(s)$ are fixed. The choice of $\delta p_r(s)$ above corresponds to an over-provisioned network. Similar relations can be derived in the under-provisioned case in terms of $p_g(s)$. The above equations can be presented in a block diagram format as depicted in Figure 1.

B. Network Controllers

In [8], a PI-type AQM was proposed as a congestion controller at core routers. This AQM was shown to be able to maintain buffer level at reference set point in the face of dynamic network conditions. Token buckets were introduced in order to maintain source throughput at a target rate $\underline{x}$. However, [10] showed that one cannot guarantee that resulting throughputs are equal to or greater than the bucket rate. To overcome this inherent limitation, [7] proposed a feedback structure around a token bucket termed ARM. The purpose of ARM is to regulate the token bucket rate A_i such that $x_i \geq \underline{x}_i$ (if the network is sufficiently provisioned). Indeed, following the ideas behind the PI-AQM, the ARM controller has the structure

$$ARM(s) = \frac{k_{arm}(\frac{s}{z_{arm}} + 1)}{s(\frac{s}{p_{arm}} + 1)}$$

and is illustrated in Figure 2. Note that ARM compares source rate to its bucket rate, hence, it is necessary to construct rate estimation. This is done using a modified TSW (Time-Slice Window) procedure [13]: the source rate estimate is computed by measuring the number of sent packets over a fixed time period T_{TSW} and further smoothed by a low-pass filter F. The transfer function representing this estimation is given by

$$F(s) = \frac{a}{s+a} e^{-sT_{TSW}}.$$

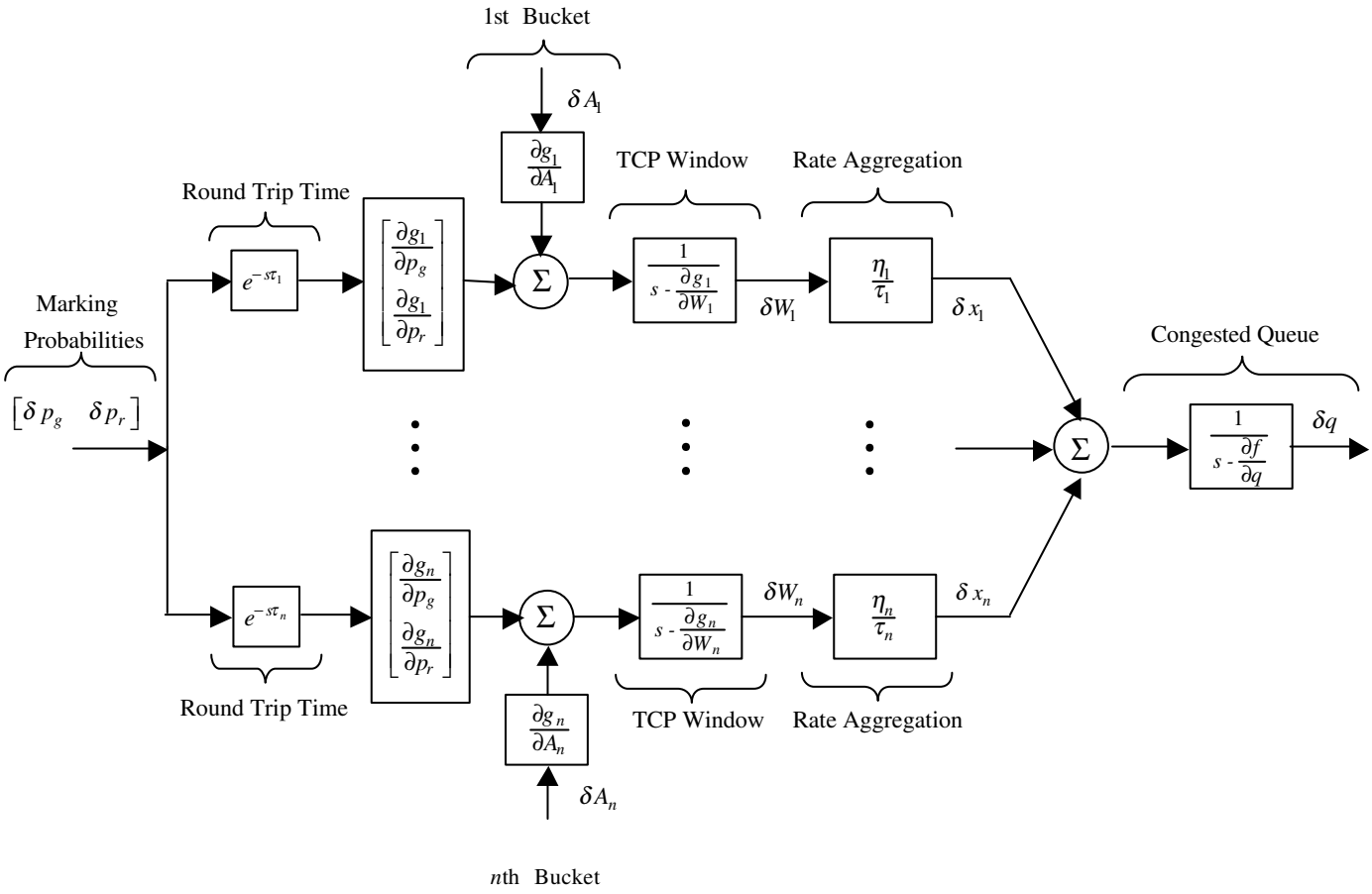

Fig. 1. Block diagram of the linearized open-loop network.

DiffServ stipulates that AQMs differentiate between green packets (those within their target rates) and red packets. The idea is to give preference to packets corresponding to sources within their target rates. We accomplish this using a multi-level PI AQM, one for green flow and a second for the red flow, along with set points, q^g_{ref} and q^r_{ref}, respectively, as shown in Figure 3. The marking probabilities, p_g and p_r, for the green and red fluid, respectively, are computed by the two PI AQM controllers, $AQM_g(s)$ and $AQM_r(s)$. Setting $q^g_{ref} > q^r_{ref}$ insures that red packets are marked before green packets [9]. We use the same controller in both loops, that is,

$$AQM(s) = AQM_g(s) = AQM_r(s) = \frac{k_{aqm}(\frac{s}{z_{aqm}} + 1)}{s}. \tag{7}$$

Combining the open-loop network model with the ARM and AQM controllers leads to the closed-loop block diagram of the DiffServ network shown in Figure 4. Next, we analyze local stability of this network.

IV. Stability of DiffServ Networks

In this section, we discuss the effect of ARM on stability of the DiffServ network. The network's linearized model, shown in Figure 4, comprises of n heterogeneous TCP sources with n ARM loops. We now present our main result.

Theorem: *Consider the linearized DiffServ network shown in Figure 4. There exist* AQM *and* $\{ARM_j : j = 1, \ldots, n\}$ *such that the system is locally stable.*

Proof. We start with a sketch of the proof. The block diagram in Figure 4 is redrawn in Figure 5 to show a nominal (i.e., without ARMs) TCP/AQM network along with perturbations due to active ARMs. A network we comprises of n heterogeneous TCP sources with m active ARM loops (see Appendix B), where $m < n$ (see [14]). The set of active ARM loops is defined by $J \triangleq \{1 \leq j \leq n : \ j^{th}$ ARM loop is active at equilibrium$\}$.

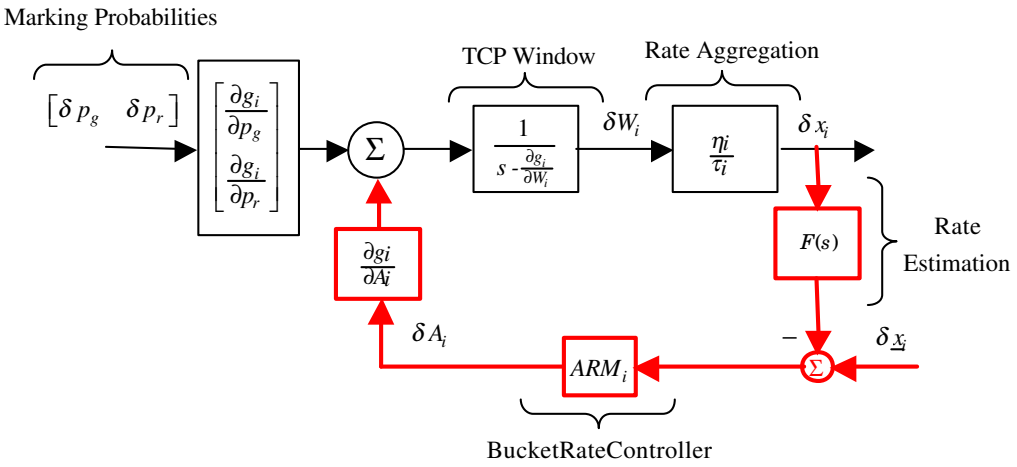

Fig. 2. The ARM controller.

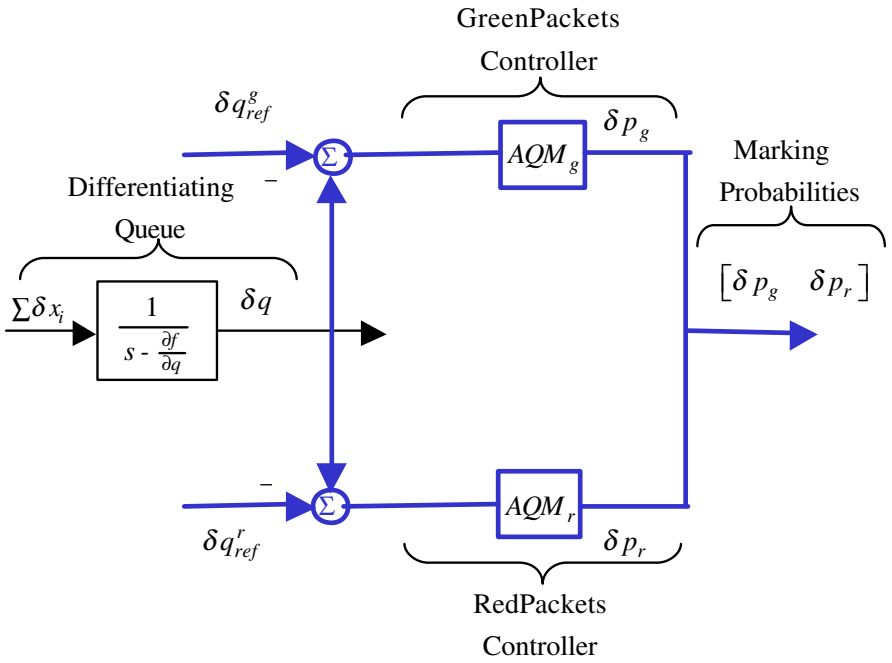

Fig. 3. The multi-level AQM control system.

That is, if $ARM_i = 0, i = 1, \ldots, n$, then the block diagram reduces to a series connection between the open-loop network in Figure 1 and the AQM (albeit single controller) in Figure 3. These perturbations can be combined into a single block as shown in Figure 6. We then apply small gain arguments to establish closed-loop stability.

The nominal TCP/AQM system in Figure 5, denoted by $\hat{P}$, is described by

$$\hat{P}(s) \triangleq \frac{\delta p}{\delta \hat{x}} = \frac{\frac{1}{s-\frac{\partial f}{\partial q}} AQM}{1 - \frac{1}{s-\frac{\partial f}{\partial q}} AQM \sum_{i=1}^{n} P_i}, \tag{8}$$

where $\delta\tilde{x}$ is the total rate perturbation from nominal TCP/AQM value due to active ARMs:

$$\delta\hat{x} = \sum_{i \in J} \delta\hat{x}_i, \quad \delta\hat{x}_i = P_i \Delta_i \delta p.$$

The source's TCP transfer function P_i is given by

$$P_i = e^{-s\tau_i} \frac{\partial g_i}{\partial p} \frac{1}{s - \frac{\partial g_i}{\partial W_i}} \frac{\eta_i}{\tau_i},$$

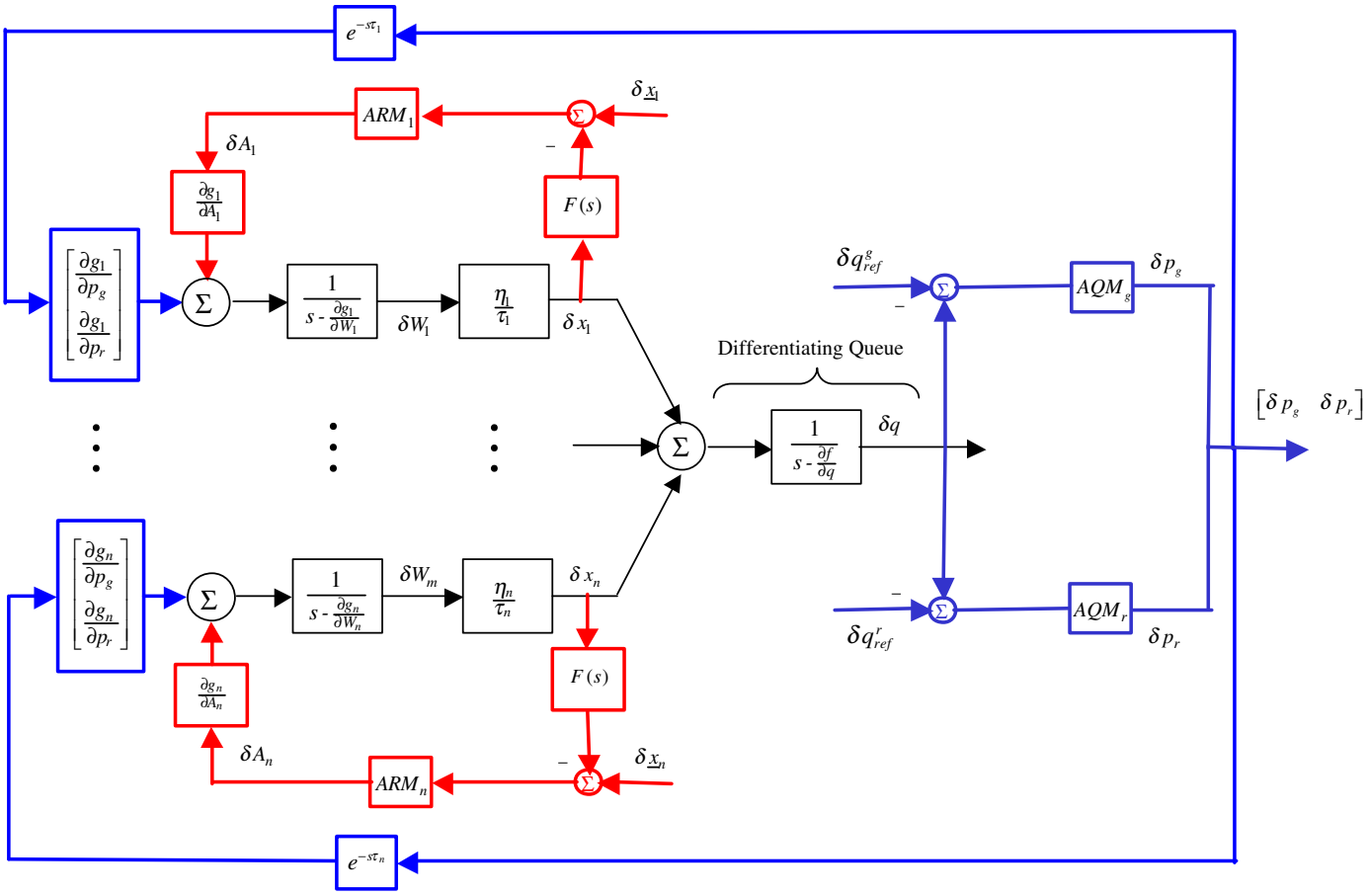

Fig. 4. The combined ARM/AQM DiffServ network.

with ARM-induced perturbation $\Delta_j(s)$:

$$\Delta_j(s) = \frac{\frac{1}{s-\frac{\partial g_j}{\partial W_j}} \frac{\eta_j}{\tau_j} \frac{\partial g_j}{\partial A_j} ARM_j \cdot F_j(s)}{1 + \frac{1}{s-\frac{\partial g_j}{\partial W_j}} \frac{\eta_j}{\tau_j} \frac{\partial g_j}{\partial A_j} ARM_j \cdot F_j(s)}.$$

Note that due to the Δ_i block, the marking probability δu_i experienced by a source with an active ARM is different from the AQM's δp. Finally, a simplified formulation of this system with a single perturbation block Δ is shown in Figure 6 where

$$\Delta(s) = \sum_{j \in J} P_j \Delta_j(s),$$

Next, we derive upper bounds on the AQM and ARM gains guaranteeing stability of $\hat{P}$ and Δ, then provide additional bounds on these gains such that $\|\hat{P}\Delta\|_\infty < 1$. These gain constraints are used to show that the system in Figure 6 is stable which implies stability of the system in Figure 4.

To analyze stability of Δ it is sufficient to discuss stability of Δ_j as follows. We use Nyquist stability criteria to show that there exists $k_{arm_j} > 0$ stabilizing Δ_j. Δ_j can be written as this closed-loop system

$$\Delta_j(s) = \frac{L_{\Delta_j}(s)}{1 + L_{\Delta_j}(s)}$$

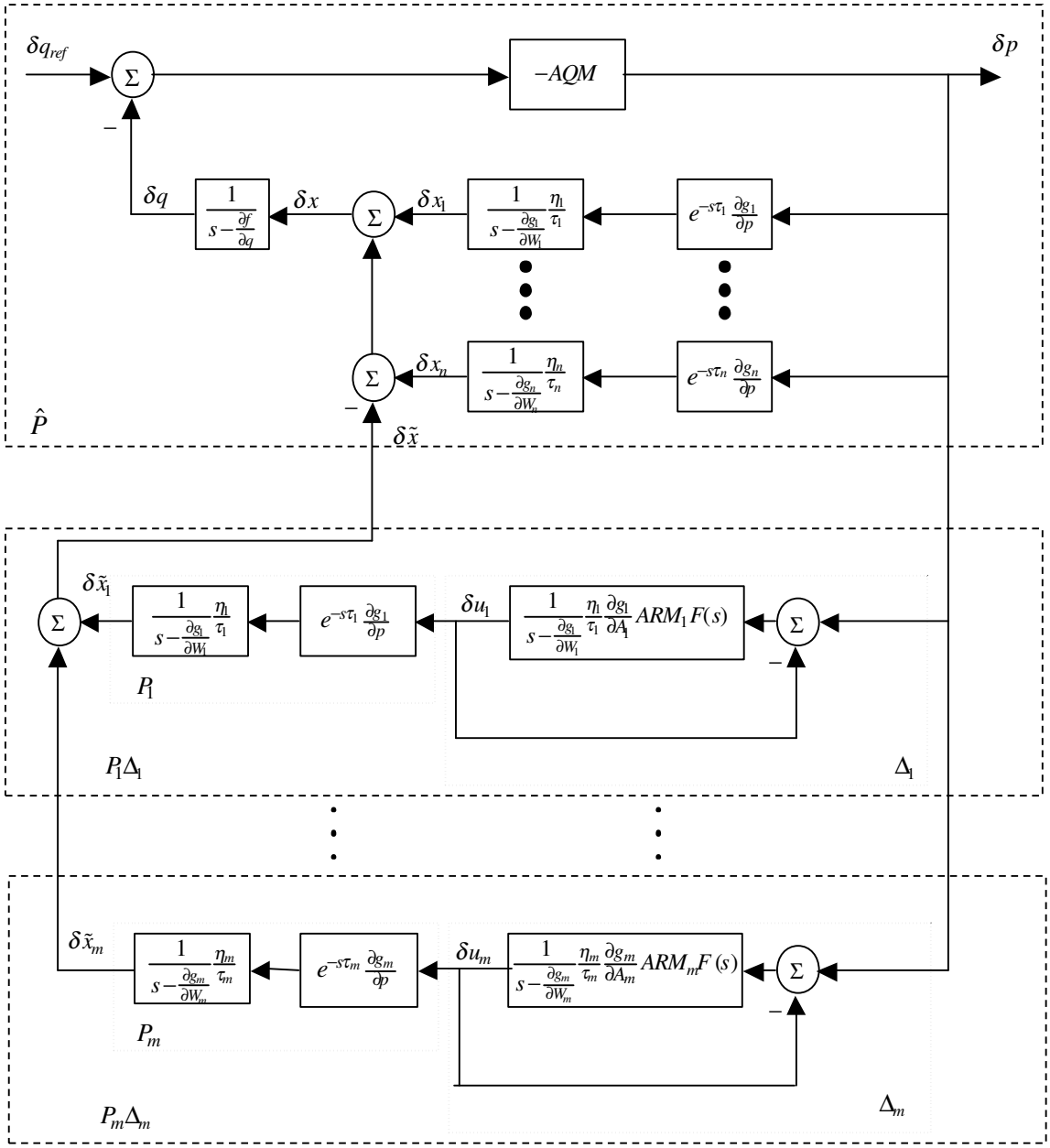

Fig. 5. Block diagram of AQM networks with active ARM loops (the perturbation blocks indexes correspond to those in the set J) .

where $L_{\Delta_j}(s)$ is given by

$$\begin{aligned} L_{\Delta_j}(s) &= \frac{1}{s-\frac{\partial g_j}{\partial W_j}}\frac{\eta_j}{\tau_j}\frac{\partial g_j}{\partial A_j}ARM_jF_j(s) \\ &= \frac{1}{s-\frac{\partial g_j}{\partial W_j}}\frac{\eta_j}{\tau_j}\frac{\partial g_j}{\partial A_j}\frac{k_{arm_j}(\frac{s}{z_{arm_j}}+1)}{s(\frac{s}{p_{arm_j}}+1)}\frac{a_j}{s+a_j}e^{-sT_{TSW_j}}. \end{aligned} \tag{9}$$

Since $L_{\Delta_j}(s)$ has a pole at the origin, it is necessary that the Nyquist contour Γ includes an infinitesimal semicircle Γ_ϵ around $s=0$ described by (see Figure 7(a))

$$\Gamma_\epsilon \triangleq \{s=\epsilon e^{j\theta};\ \ \theta\in[-90^\circ,90^\circ],\ \epsilon\to 0,\ \epsilon>0\} \tag{10}$$

As s traverses from $-j\epsilon$ to $+j\epsilon$ along Γ_ϵ, θ changes from -90° to $+90^\circ$ counterclockwise. The corresponding

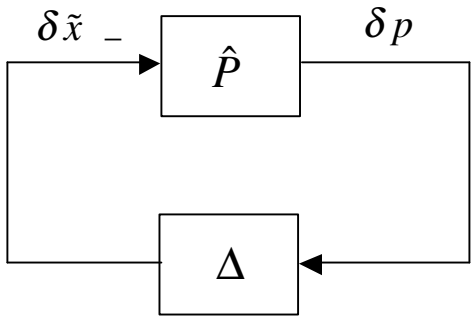

Fig. 6. Simplified block diagram of the system in Figure 5.

Nyquist plot of $L_{\Delta_j}(s)$ can be determined by evaluating (9) along (10). In the limit we have,

$$\lim_{\epsilon\to 0} L_{\Delta_j}(\epsilon e^{j\theta}) = \frac{1}{-\frac{\partial g_j}{\partial W_j}} \frac{\eta_j}{\tau_j} \frac{\partial g_j}{\partial A_j} \frac{k_{arm_j}}{\epsilon e^{j\theta}}.$$

The contour indentation near the origin Γ_ϵ is mapped by $L_{\Delta_j}(s)$ into a semi-infinite circle covering the RHP of the complex plane. The generic Nyquist plot in Figure 7(b), which preserves its form no matter the magnitude of $k_{arm_j} > 0$, is similar to that of our $L_{\Delta_j}(s)$. Any instabilities in $\Delta_j(s)$ will be a result of encirclements by the Nyquist plot of $L_{\Delta_j}(s)$ over the range $\omega \in (\epsilon, +\infty) \cup (-\epsilon, -\infty)$. Define $L_{\Delta_j}(j\omega) = k_{arm_j}\tilde{L}_{\Delta_j}(j\omega)$. The plot of $\tilde{L}_{\Delta_j}(j\omega)$ crosses the negative real-axis at frequencies in the set $\Omega = \{\omega : \angle\tilde{L}_{\Delta_j}(j\omega) = -180°\}$. Let ω_1 be the frequency such that $|\tilde{L}_{\Delta_j}(j\omega_1)| = \max_{\omega\in\Omega}|\tilde{L}_{\Delta_j}(j\omega)|$. If $k_{arm_j} < |\tilde{L}_{\Delta_j}(j\omega_1)|^{-1}$ then $|L_{\Delta_j}(j\omega)| < 1$ implying stability of Δ_j. Stability of Δ follows immediately from

$$k_{arm_j} < \frac{1}{|\tilde{L}_{\Delta_j}(j\omega_1)|}, \quad j = 1, \ldots, n. \tag{11}$$

We follow a similar procedure to derive an upper bound on the AQM gain sufficient to stabilize $\hat{P}$. The details

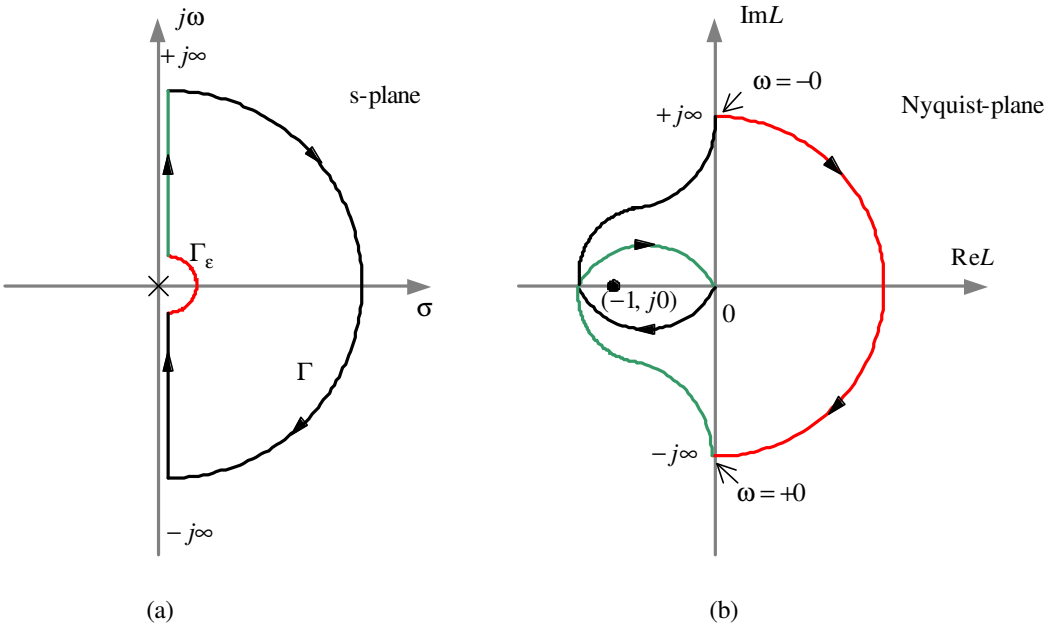

Fig. 7. (a) The Nyquist contour Γ_ϵ (b) A generic Nyquist plot of open loop transfer function $L(s)$.

are shown in Appendix C.

Next, we show that $|\hat{P}(j\omega)\Delta(j\omega)| < 1$ over the ranges $[0, \omega_0]$ and $[\omega_0, \infty]$, where ω_0 is a sufficiently small frequency to be defined later. To this end, we now show that $\|\Delta_j(s)\|_\infty = 1$ which is used later. Let $Re(L_{\Delta_j}(j\omega))$

denote the real part of $L_{\Delta_j}(j\omega)$ and let ω_2 be the frequency where $Re(\tilde{L}_{\Delta_j}(j\omega_2)) = \min_{\omega\in\Gamma} Re(\tilde{L}_{\Delta_j}(j\omega))$. Hence, $Re(L_{\Delta_j}(j\omega)) > -\frac{1}{2}$ if $k_{arm_j} < 2|Re(\tilde{L}_{\Delta_j}(j\omega_2))|^{-1}$, or equivalently $\left|\frac{L_{\Delta_j}(j\omega)}{1+L_{\Delta_j}(j\omega)}\right| < 1$ [15]. Noting that $|\Delta_j(j\omega)| = 1$ at $\omega = 0$ (due to the integrator), we have shown that

$$\|\Delta_j(j\omega)\|_\infty = 1 \Longrightarrow k_{arm_j} < \min\left\{\frac{1}{2|Re(\tilde{L}_{\Delta_j}(j\omega_2)|}, \frac{1}{|\tilde{L}_{\Delta_j}(j\omega_1)|}\right\}. \tag{12}$$

Now consider the product $|\hat{P}(j\omega)\Delta(j\omega)|$ over the range $\omega \in [0, \omega_0]$. First, we bound Δ using

$$\begin{aligned} |\Delta(j\omega)| &= \left|\sum_{j\in J} P_j(j\omega)\Delta_j(j\omega)\right| \leq \sum_{j\in J} |P_j(j\omega)\Delta_j(j\omega)| \\ &= \sum_{j\in J} |P_j(j\omega)||\Delta_j(j\omega)| \leqslant \sum_{j\in J} |P_j(j\omega)|. \end{aligned} \tag{13}$$

Then we rewrite $\hat{P}$ in terms of $\sum_{j\in J} |P_j(j\omega)|$

$$\hat{P} = \left|\frac{\frac{1}{j\omega - \frac{\partial f}{\partial q}} AQM(\sum_{i=1}^n P_i(j\omega))}{1 - \frac{1}{j\omega - \frac{\partial f}{\partial q}} AQM(\sum_{i=1}^n P_i(j\omega))}\right| \left|\frac{1}{\sum_{i=1}^n P_i(j\omega)}\right|$$

and show that

$$\left\|\frac{\frac{1}{j\omega - \frac{\partial f}{\partial q}} AQM(\sum_{i=1}^n P_i(j\omega))}{1 - \frac{1}{j\omega - \frac{\partial f}{\partial q}} AQM(\sum_{i=1}^n P_i(j\omega))}\right\|_\infty = \left\|\frac{L_{\hat{P}}(j\omega)}{1 + L_{\hat{P}}(j\omega)}\right\|_\infty = 1.$$

At $\omega = 0$, due to the AQM's integrator

$$\left|\frac{\frac{1}{j\omega - \frac{\partial f}{\partial q}} AQM(\sum_{i=1}^n P_i(j\omega))}{1 - \frac{1}{j\omega - \frac{\partial f}{\partial q}} AQM(\sum_{i=1}^n P_i(j\omega))}\right| = 1.$$

Let $Re(L_{\hat{P}}(j\omega))$ denote the real part of $L_{\hat{P}}(j\omega)$ with the factorization $Re(L_{\hat{P}}(j\omega)) = k_{aqm} Re(\tilde{L}_{\hat{P}}(j\omega))$. Let ω_3 be the frequency where $Re(\tilde{L}_{\hat{P}}(j\omega_3)) = \min_{\omega\in\Gamma} Re(\tilde{L}_{\hat{P}}(j\omega))$. Hence, $Re(L_{\hat{P}}(j\omega)) > -\frac{1}{2}$ if $k_{aqm} < 2|Re(\tilde{L}_{\hat{P}}(j\omega_3))|^{-1}$, or equivalently, $\left|\frac{L_{\hat{P}}(j\omega)}{1+L_{\hat{P}}(j\omega)}\right| < 1$ [15]. This proves that

$$k_{aqm} < \frac{1}{2|Re(\tilde{L}_{\hat{P}}(j\omega_3))|} \Longrightarrow \left\|\frac{\frac{1}{j\omega - \frac{\partial f}{\partial q}} AQM(\sum_{i=1}^n P_i(j\omega))}{1 - \frac{1}{j\omega - \frac{\partial f}{\partial q}} AQM(\sum_{i=1}^n P_i(j\omega))}\right\|_\infty = 1. \tag{14}$$

It follows from (14) that

$$\begin{aligned} |\hat{P}(j\omega)| &= \left|\frac{\frac{1}{j\omega - \frac{\partial f}{\partial q}} AQM}{1 - \frac{1}{j\omega - \frac{\partial f}{\partial q}} AQM(\sum_{i=1}^n P_i(j\omega))}\right| \\ &= \left|\frac{\frac{1}{j\omega - \frac{\partial f}{\partial q}} AQM(\sum_{i=1}^n P_i(j\omega))}{1 - \frac{1}{j\omega - \frac{\partial f}{\partial q}} AQM(\sum_{i=1}^n P_i(j\omega))}\right| \left|\frac{1}{\sum_{i=1}^n P_i(j\omega)}\right| \\ &\leq \left|\frac{1}{\sum_{i=1}^n P_i(j\omega)}\right|. \end{aligned} \tag{15}$$

Combining (13)-(15) we obtain

$$|\hat{P}(j\omega)\Delta(j\omega)| = |\hat{P}(j\omega)||\Delta(j\omega)| \leqslant \frac{\sum_{j\in J} |P_j(j\omega)|}{|\sum_{i=1}^n P_i(j\omega)|}. \tag{16}$$

We observe that the right-hand side of (16) is a continuous function of ω, and at $\omega = 0$ it is smaller than 1. Thus, given any $0 < \epsilon_1 \ll 1$, there exists a sufficiently small frequency ω_0, such that

$$\left| \frac{\sum_{j\in J} |P_j(j\omega)|}{|\sum_{i=1}^n P_i(j\omega)|} - \frac{\sum_{j\in J} |P_j(j0)|}{|\sum_{i=1}^n P_i(j0)|} \right| \leq \epsilon_1, \ |\omega - 0| \leq \omega_0.$$

Hence

$$\left| \frac{\sum_{j\in J} |P_j(j\omega)|}{|\sum_{i=1}^n P_i(j\omega)|} \right| < 1, \ \forall \omega \in [0, \omega_0].$$

and we proved that if k_{aqm} stabilizes $\hat{P}$ (see Appendix C) and satisfies (14), then

$$|\hat{P}(j\omega)\Delta(j\omega)| < 1, \ \forall \omega \in [0, \omega_0]. \tag{17}$$

Finally, we show that $|\hat{P}(j\omega)\Delta(j\omega)| < 1$ over $\omega \in [\omega_0, \infty)$. $|L(j\omega)|$ in (24) can be expanded as follows

$$\begin{aligned}
|L(j\omega)| &= \left| -\frac{1}{j\omega - \frac{\partial f}{\partial q}} \frac{k_{aqm}(\frac{j\omega}{z_{aqm}} + 1)}{j\omega} \sum_{i=1}^n e^{-j\omega\tau_i} \frac{\partial g_i}{\partial p} \frac{1}{j\omega - \frac{\partial g_i}{\partial W_i}} \frac{\eta_i}{\tau_i} \right| \\
&= \left| \frac{1}{j\omega - \frac{\partial f}{\partial q}} \right| \left| \frac{k_{aqm}(\frac{j\omega}{z_{aqm}} + 1)}{j\omega} \right| \left| \sum_{i=1}^n e^{-j\omega\tau_i} \frac{\partial g_i}{\partial p} \frac{1}{j\omega - \frac{\partial g_i}{\partial W_i}} \frac{\eta_i}{\tau_i} \right| \\
&\leq \left| \frac{1}{j\omega - \frac{\partial f}{\partial q}} \right| \left| \frac{k_{aqm}(\frac{j\omega}{z_{aqm}} + 1)}{j\omega} \right| \sum_{i=1}^n \left| e^{-j\omega\tau_i} \frac{\partial g_i}{\partial p} \frac{1}{j\omega - \frac{\partial g_i}{\partial W_i}} \frac{\eta_i}{\tau_i} \right| \\
&= \left| \frac{1}{j\omega - \frac{\partial f}{\partial q}} \right| \left| \frac{k_{aqm}(\frac{j\omega}{z_{aqm}} + 1)}{j\omega} \right| \sum_{i=1}^n |e^{-j\omega\tau_i}| \left| \frac{\partial g_i}{\partial p} \right| \left| \frac{1}{j\omega - \frac{\partial g_i}{\partial W_i}} \right| \left| \frac{\eta_i}{\tau_i} \right|.
\end{aligned}$$

At $\omega \geq \omega_0$,

$$\begin{aligned}
|L(j\omega)| &< \left| \frac{1}{\omega_0} \right| \left| \frac{k_{aqm}(\frac{j\omega}{z_{aqm}} + 1)}{j\omega} \right| \sum_{i=1}^n \left| \frac{\partial g_i}{\partial p} \right| \left| \frac{1}{\omega_0} \right| \left| \frac{\eta_i}{\tau_i} \right| \\
&= \left| \frac{1}{\omega_0} \right| \left| \frac{k_{aqm}}{z_{aqm}} - \frac{k_{aqm}}{\omega} j \right| \sum_{i=1}^n \left| \frac{\partial g_i}{\partial p} \right| \left| \frac{1}{\omega_0} \right| \left| \frac{\eta_i}{\tau_i} \right| \\
&= \left| \frac{1}{\omega_0} \right| \left| k_{aqm} \sqrt{\left(\frac{1}{z_{aqm}}\right)^2 + \left(\frac{1}{\omega}\right)^2} \right| \sum_{i=1}^n \left| \frac{\partial g_i}{\partial p} \right| \left| \frac{1}{\omega_0} \right| \left| \frac{\eta_i}{\tau_i} \right| \\
&\leq \left| \frac{1}{\omega_0} \right| \left| k_{aqm} \sqrt{\left(\frac{1}{z_{aqm}}\right)^2 + \left(\frac{1}{\omega_0}\right)^2} \right| \sum_{i=1}^n \left| \frac{\partial g_i}{\partial p} \right| \left| \frac{1}{\omega_0} \right| \left| \frac{\eta_i}{\tau_i} \right| \\
&\triangleq M k_{aqm} < \infty.
\end{aligned}$$

Hence, over the range $\omega \in [\omega_0, \infty)$

$$k_{aqm} < \frac{\epsilon_2}{M} \Longrightarrow |L(j\omega)| < \epsilon_2. \tag{18}$$

From (18)

$$|\hat{P}(j\omega)| = \left| \frac{\frac{1}{j\omega - \frac{\partial f}{\partial q}} AQM}{1 - \frac{1}{j\omega - \frac{\partial f}{\partial q}} AQM(\sum_{i=1}^n P_i)} \right| < \left| \frac{\frac{1}{j\omega - \frac{\partial f}{\partial q}} AQM}{1 - \epsilon_2} \right| = \left| \frac{\frac{1}{j\omega - \frac{\partial f}{\partial q}} \frac{k_{aqm}(\frac{j\omega}{z_{aqm}} + 1)}{j\omega}}{1 - \epsilon_2} \right|.$$

and to bound $|\hat{P}|$ consider the product

$$\begin{aligned} m\left|\frac{k_{max}}{j\omega+p_{min}}\right||\hat{P}(j\omega)| &< m\left|\frac{k_{max}}{j\omega+p_{min}}\right|\left|\frac{1}{j\omega-\frac{\partial f}{\partial q}}\right|\left|\frac{k_{aqm}(\frac{j\omega}{z_{aqm}}+1)}{j\omega}\right|\left|\frac{1}{1-\epsilon_2}\right| \\ &< (n-1)\left|\frac{k_{max}}{\omega_0}\right|\left|\frac{1}{\omega_0}\right|\left|k_{aqm}\sqrt{\left(\frac{1}{z_{aqm}}\right)^2+\left(-\frac{1}{\omega_0}\right)^2}\right|\left|\frac{1}{1-\epsilon_2}\right| \\ &\triangleq \tilde{M}k_{aqm}<\infty, \end{aligned}$$

where $k_{max} \triangleq \max_{j\in J}\left\{\left|\frac{\partial g_j}{\partial p}\frac{\eta_j}{\tau_j}\right|\right\}$ and $p_{min} \triangleq \min_{j\in J}\left\{-\frac{\partial g_j}{\partial W_j}\right\}$. This proves that over the range $\omega \in [\omega_0, \infty)$

$$k_{aqm} < \min\left\{\frac{\epsilon_1}{M}, \frac{1}{\tilde{M}}\right\} \Longrightarrow |\hat{P}(j\omega)| < \frac{1}{m\left|\frac{k_{max}}{j\omega+p_{min}}\right|}. \tag{19}$$

Evaluating $|\Delta|$ over $\omega \in [\omega_0, \infty)$ gives

$$\begin{aligned} |\Delta| &\leq \sum_{j\in J}|P_j||\Delta_j| \leq \sum_{j\in J}|P_j| = \sum_{j\in J}\left|e^{-j\omega\tau_j}\frac{\partial g_j}{\partial p}\frac{1}{j\omega-\frac{\partial g_j}{\partial W_j}}\frac{\eta_j}{\tau_j}\right| \\ &\leq \sum_{j\in J}\left|\frac{k_{max}}{j\omega+p_{min}}\right| = (n-1)\left|\frac{k_{max}}{j\omega+p_{min}}\right|, \end{aligned} \tag{20}$$

and combining (19) and (20) results in

$$k_{aqm} < \min\left\{\frac{\epsilon_1}{M}, \frac{1}{\tilde{M}}\right\} \Longrightarrow |\hat{P}(j\omega)\Delta(j\omega)| < 1,\ \forall\omega \in [\omega_0, \infty). \tag{21}$$

Finally, if the ARMs gains are bounded by (12)

$$k_{arm_j} < \min\left\{\frac{1}{2|Re(\tilde{L}_{\Delta_j}(j\omega_2)|}, \frac{1}{|\tilde{L}_{\Delta_j}(j\omega_1)|}\right\},\ j = 1, \ldots, n,$$

and the AQMs gain are bounded by (17), (19), (21) and (25)

$$k_{aqm} < \min\left\{\frac{1}{2|Re(\tilde{L}_{\hat{P}}(j\omega_3))|}, \frac{\epsilon_1}{M}, \frac{1}{\tilde{M}}, \frac{1}{|\tilde{L}(j\omega_4)|}\right\}$$

then both $\hat{P}$ and Δ are stable and $\|\hat{P}(j\omega)\Delta(j\omega)\|_\infty = 1$. Hence, we have shown that the DiffServ network shown in Figure 4 is locally stable if k_{aqm} and k_{arm} satisfy their gain constraints. This proves that there exist AQM and $\{ARM_j :\ j = 1, \ldots, n\}$ such that the system is locally stable. □

V. Illustrative Examples

In this section, we apply the Theorem to analyze stability of the DiffServ network in [7]. This network consisted of three heterogeneous sources, each served by an edge with fully-coloring ARM as shown in Figure (8). The edges feed into a congested core with an admissible, compatible and non-overlapping differentiation ability (see Appendix B and [9]). The propagation delays T_{pi} are all uniform in the ranges: $T_{p1} \in [50-90]$ msec, $T_{p2} \in [15-25]$ msec and $T_{p3} \in [0-10]$ milliseconds. Each source is an aggregate of η_i generic FTP flows, all starting uniformly in $[0, 50]$ sec, with loads $\eta_1 = 20$, $\eta_2 = 30$ and $\eta_3 = 25$. The core queue has a buffer size of 800 packets and ECN marking enabled. The source target rates are $\underline{x}_1 = 2000$, $\underline{x}_2 = 500$ and $\underline{x}_3 = 1250$ packet/second.

The same AQM controller was used for green and red flows and is given by

$$AQM(s) = \frac{9.6\times10^{-6}(\frac{s}{0.53}+1)}{s}.$$

The set points for the red and green controllers were $q^r_{ref} = 100$ packets and $q^g_{ref} = 250$ packets. The idea behind this choice is while fully utilizing the link also minimize the possibility of the queue oscillating between these points due to incoming flow bursts.

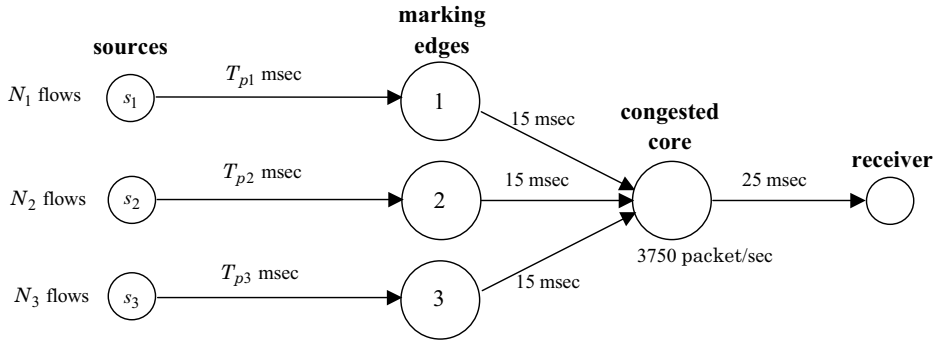

Fig. 8. The simulated DiffServ network.

In [7], the ARMs are the same where

$$ARM_j(s) = \frac{0.05(\frac{s}{0.1}+1)}{s(s+1)};\ j = 1, 2, 3.$$

The source rate estimator implements the modified TSW algorithm with the three buckets using $T_{TSW} = 1$ second. It is further smoothed by a first-order, low-pass filter with a corner frequency of $a = 1$ rad/second with the transfer function $F(s)$ of

$$F(s) = \frac{1}{s+1}e^{-s}.$$

We analyze stability of two implementations, an over-provisioned and an under-provisioned network.

A. Over-Provisioned Network

In the over-provisioned case, the link capacity is $c = 4500$ packets/second. In Appendix B it is shown that the queue length at equilibrium is at $q^r_{ref} = 100$ packets with $p_r < 1$, $p_g = 0$. Hence, the round trip times are $\tau_1 = 0.2422$ second, $\tau_2 = 0.1422$ second and $\tau_3 = 0.1122$ second. According to [14], $\frac{x_1}{\alpha_1} > \frac{x_3}{\alpha_3} > \frac{x_2}{\alpha_2}$, where $\alpha_i = \frac{\eta_i}{\tau_i}$. We also compute $i^* = 2$ (see [14]) implying that the second and the third ARMs are de-activated and $J = \{1\}$. The generalized system block diagram in Figure 5 can be reduced in this case to the one shown in Figure 9 where the nominal TCP/AQM system is described by

$$\hat{P}(s) = \frac{\delta\hat{x}_1}{\delta p_r} = \frac{\frac{1}{s-\frac{\partial f}{\partial q}}AQM}{1 - \frac{1}{s-\frac{\partial f}{\partial q}}AQM(\sum_{i=1}^{3} P_i)},$$

where $\frac{\partial f}{\partial q} = -5.0914$ 1/second; and where the transfer functions for the individual sources are described by

$$\begin{aligned} P_1(s) &= e^{-s\tau_1}\frac{\partial g_1}{\partial p_r}\frac{1}{s-\frac{\partial g_1}{\partial W_1}}\frac{\eta_1}{\tau_1} \\ &= e^{-s(0.2422)}(-72.9144)\frac{1}{s-(-3.0248)}\frac{20}{0.2422}; \end{aligned}$$

$$\begin{aligned} P_2(s) &= e^{-s\tau_2}\frac{\partial g_2}{\partial p_r}\frac{1}{s-\frac{\partial g_2}{\partial W_2}}\frac{\eta_2}{\tau_2} \\ &= e^{-s(0.1422)}(-26.7843)\frac{1}{s-(-0.9483)}\frac{30}{0.1422}; \end{aligned}$$

$$\begin{aligned} P_3(s) &= e^{s\tau_3}\frac{\partial g_3}{\partial p_r}\frac{1}{s-\frac{\partial g_3}{\partial W_3}}\frac{\eta_3}{\tau_3} \\ &= e^{-s(0.1122)}(-149.1887)\frac{1}{s-(-2.8450)}\frac{25}{0.1122}. \end{aligned}$$

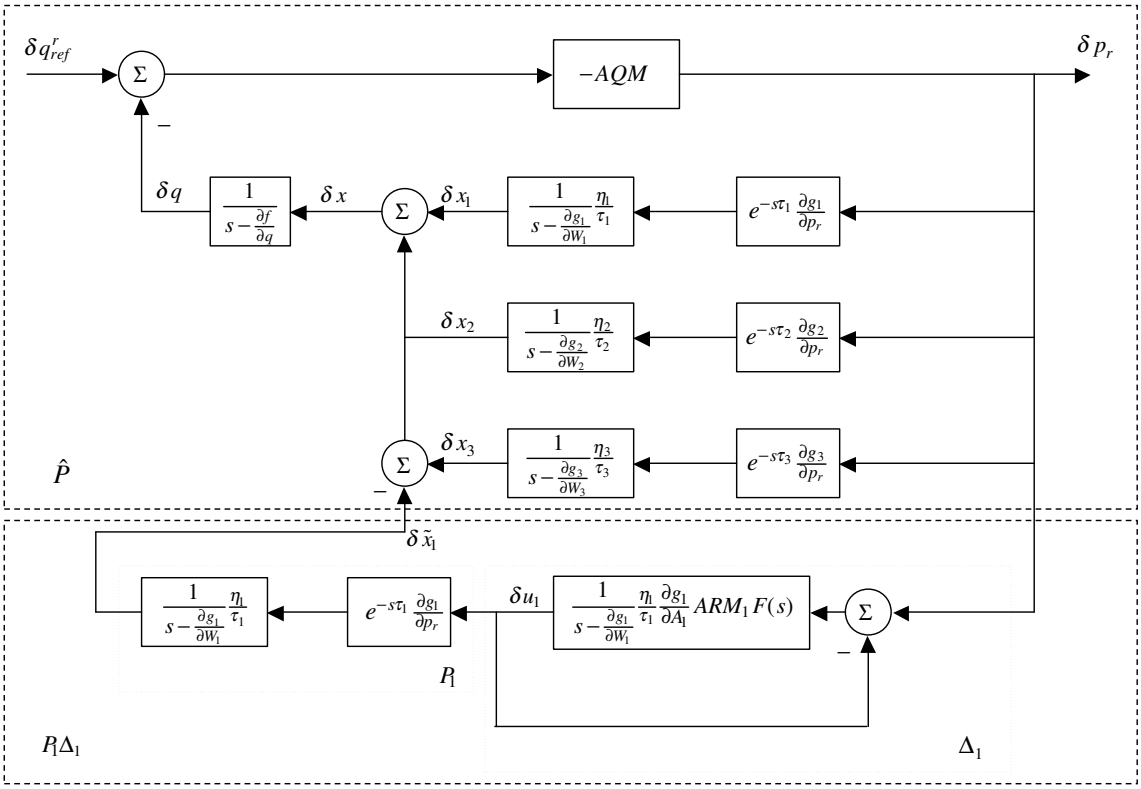

Fig. 9. Block diagram of the over-provisioned network.

We observe in Figure 10 that $\|\hat{P}\Delta\|_\infty < 1$, which along with stability of $\hat{P}$ and Δ (not shown here) establishes local stability of this DiffServ network. Further details and simulation plots can be found in [9].

B. Under-Provisioned Network

In this setup, the link capacity is 20% under provisioned where $c = 3000$ packets/second. From Appendix B, it follows that $p_r = 1, 0 < p_g < 1$,and $q = q^g_{ref} = 250$ packets. The round trip times are $\tau_1 = 0.3033$ second, $\tau_2 = 0.2033$ second and $\tau_3 = 0.1733$ second. According to [14], $\frac{x_1}{\alpha_1} > \frac{x_3}{\alpha_3} > \frac{x_2}{\alpha_2}$ and $i^* = 1$, implying that the first ARM is de-activated and $J = \{2, 3\}$. The generalized system block diagram in Figure 5 can be reduced in this case to the one shown in Figure 11 where the nominal TCP/AQM system is described by

$$\hat{P}(j\omega) = \frac{\delta\hat{x}}{\delta p_g} = \frac{\frac{1}{j\omega - \frac{\partial f}{\partial q}} AQM}{1 - \frac{1}{j\omega - \frac{\partial f}{\partial q}} AQM(\sum_{i=1}^{3} P_i)},$$

where $\frac{\partial f}{\partial q} = -4.5971$ 1/second; and where the transfer functions for the individual sources are described by

$$\begin{aligned} P_1 &= \frac{\delta x_1}{\delta p_g} = e^{-j\omega\tau_1}\frac{\partial g_1}{\partial p_g}\frac{1}{j\omega - \frac{\partial g_1}{\partial W_1}}\frac{\eta_1}{\tau_1} \\ &= e^{-j\omega(0.3033)}(-595.7)\frac{1}{j\omega - (-31.59)}\frac{20}{0.3033}; \end{aligned}$$

$$\begin{aligned} P_2 &= \frac{\delta x_2}{\delta p_g} = e^{-j\omega\tau_2}\frac{\partial g_2}{\partial p_g}\frac{1}{j\omega - \frac{\partial g_2}{\partial W_2}}\frac{\eta_2}{\tau_2} \\ &= e^{-j\omega(0.2033)}(-33.16)\frac{1}{j\omega - (-9.822)}\frac{30}{0.2033}; \end{aligned}$$

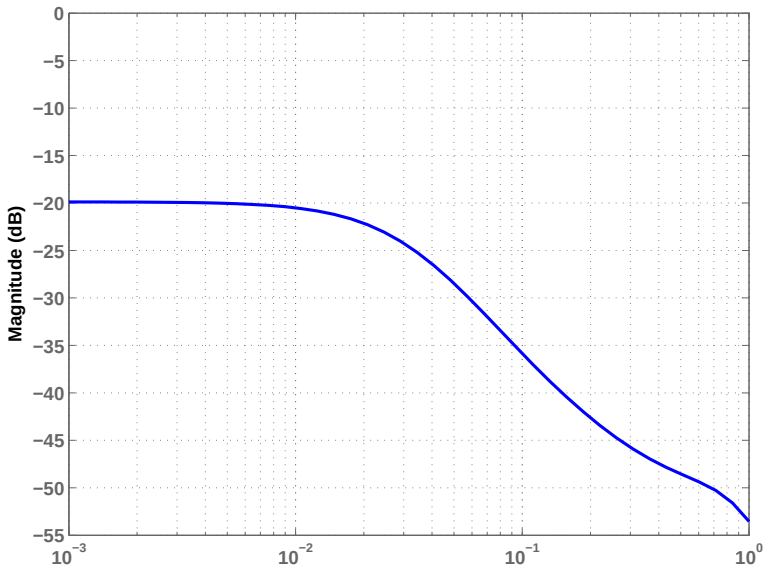

Fig. 10. The magnitude Bode plot of $\hat{P}\Delta$ (over-provisioned case).

$$\begin{aligned} P_3 &= \frac{\delta x_3}{\delta p_g} = e^{-j\omega\tau_3}\frac{\partial g_3}{\partial p_g}\frac{1}{j\omega - \frac{\partial g_3}{\partial W_3}}\frac{\eta_3}{\tau_3} \\ &= e^{-j\omega(0.1733)}(-222.4)\frac{1}{j\omega-(-25.8)}\frac{25}{0.1733}. \end{aligned}$$

Similarly to the over-provisioned case, we observe in Figure 12 that $\|\hat{P}\Delta\|_\infty < 1$, which along with stability of $\hat{P}$ and Δ (not shown here) establishes local stability of this DiffServ network. Further details and simulation plots can be found in [7].

VI. Conclusions

We analyzed stability of DiffServ networks with heterogeneous TCP flows consisting of two-level edge coloring using a token bucket, and preferentially-dropping core router. We have shown, in terms of gain bounds, the existence of AQM and ARM controllers which stabilize the network. This stability result complements our earlier work in [7] which described ns implementations and current work in [9] which quantified behavior of bucket-rate adaptation and preferential dropping that guarantees minimum throughput to users under general congestion control sources. We are presently working on generalization of this DiffServ architecture to networks with multiple congested cores.

Appendix A: Linearization

We follow the design philosophy used in [8] and design controllers based on linearized dynamics. For simplicity, at equilibrium $(q^e, {W_i}^e, {p_g}^e, {p_r}^e, {A_i}^e)$, we use $q^e = q$ and so on. We have

$$\begin{aligned} 0 &= -C + \sum_{i=1}^{n}\frac{\eta_i W_i}{\tau_i} \\ 0 &= 1 - \left(\frac{A_i}{x_i}p_g + (1-\frac{A_i}{x_i})p_r\right) - 0.5\left(\frac{A_i}{x_i}p_g + (1-\frac{A_i}{x_i})p_r\right)W_i^2 \\ \tau_i &= T_{pi} + \frac{q}{C}. \end{aligned}$$

The linearization relies on two key approximations. First, we ignore the nested delay in the term $W(t-\tau)/\tau(t-\tau)$, which is reasonable and motivated in [8]. Secondly, we assume that $\min\left\{1, \frac{A_i}{x_i}\right\} = \frac{A_i}{x_i}$, which can be enforced by

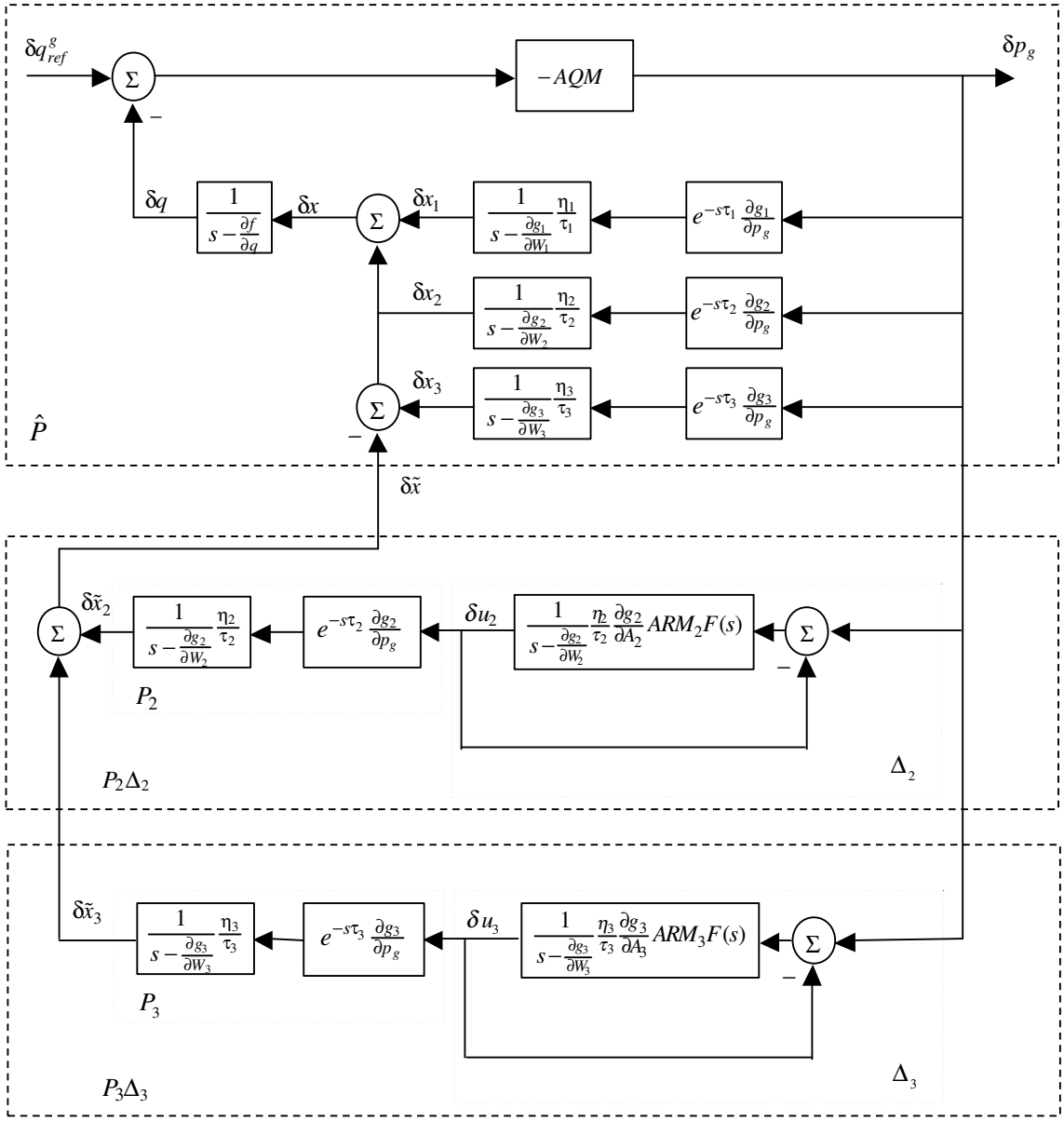

Fig. 11. Block diagram of the under-provisioned network.

the ARM controller. Otherwise, at 1 or 0 the ARM loop is deactivated. Linearization about equilibrium gives

$$\begin{aligned}\dot{\delta q}(t) &= \sum_{i=1}^{n}\frac{\partial f}{\partial W_i}\delta W_i(t)+\frac{\partial f}{\partial q}\delta q\\ \delta\dot{W}_i(t) &= \frac{\partial g_i}{\partial W_i}\delta W_i(t)+\frac{\partial g_i}{\partial p_g}\delta p_g(t-\tau_i)+\frac{\partial g_i}{\partial p_r}\delta p_r(t-\tau_i)+\frac{\partial g_i}{\partial A_i}\delta A_i(t)\end{aligned}$$

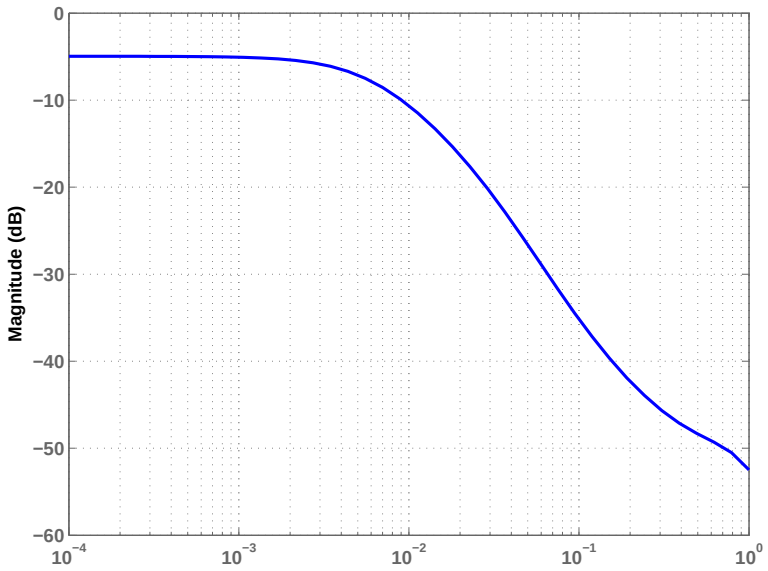

Fig. 12. The magnitude Bode plot of $\hat{P}\Delta$ (under-provisioned case).

The partial derivative terms evaluated at the operating point are given by

$$\begin{aligned}
\frac{\partial f}{\partial q} &= -\sum_{i=1}^{n} \frac{x_i}{C\tau_i} \\
\frac{\partial f}{\partial W_i} &= \frac{\eta_i}{\tau_i} \\
\frac{\partial g_i}{\partial W_i} &= \left(\frac{A_i}{\eta_i {W_i}^2} - \frac{A_i}{2\eta_i}\right)(p_g - p_r) - \frac{W_i}{\tau_i} p_r \\
\frac{\partial g_i}{\partial p_r} &= -\frac{1}{\tau_i} + \frac{A_i}{\eta_i W_i} + \frac{W_i A_i}{2\eta_i} - \frac{W_i^2}{2\tau_i} \\
\frac{\partial g_i}{\partial p_g} &= -\frac{A_i}{\eta_i W_i} - \frac{A_i W_i}{2\eta_i} \\
\frac{\partial g_i}{\partial A_i} &= -\frac{1}{\eta_i}\left(\frac{1}{W_i} + \frac{W_i}{2}\right)(p_g - p_r).
\end{aligned}$$

APPENDIX B: FIXED POINT

In [9], steady-state behavior of general DiffServ networks is investigated. Results are presented for classes of ARMs at the edge and multi-level AQM at the core that guarantee minimum throughput to users. The particular ARMs and AQMs used in this paper belong to the above classes. Several definitions and properties of the network at steady-state are used in our derivations and are presented next.

- Let $\underline{x}_i$ denote the target rate for the i-th source. We say that the router is over-provisioned if $\sum_{i=1}^{n} \underline{x}_i < c$, under-provisioned if $\sum_{i=1}^{n} \underline{x}_i > c$ and exactly-provisioned if $\sum_{i=1}^{n} \underline{x}_i = c$.
- In an under-provisioned case $\hat{q} = q^g_{ref}$, while in an over-provisioned case $\hat{q} = q^r_{ref}$.
- The marking generated by a multi-valued AQM satisfies

$$\begin{cases} \hat{p}_r < 1 \Rightarrow & \hat{p}_g = 0 \\ \hat{p}_g > 0 \Rightarrow & \hat{p}_r = 1. \end{cases} \tag{22}$$

- The coloring produced by an ARM satisfies

$$\begin{cases} \hat{x}_i < \underline{x}_i & \Rightarrow \quad \hat{f}_{gi} = 1 \\ \hat{x}_i > \underline{x}_i & \Rightarrow \quad \hat{f}_{gi} = 0. \end{cases} \tag{23}$$

- In an over-provisioned network, some sources achieve $x_i > \underline{x}_i$, hence, due to the integrators in the ARM_i, we have $A_i = 0$, We say that these ARM loops are *deactivated*. All other ARM loops are said to be *active*. In an under provisioned network, some sources achieve $x_i < \underline{x}_i$, due to the integrators in the classes ARM_i, $A_i \to \infty$. We say that these ARM loops are deactivated. All other ARM loops are said to be active. Small changes about equilibrium will not cause a change in $\hat{A}_i$, hence, active and deactivated ARM loops remain the same and the linearization still holds.

APPENDIX C: STABILITY OF $\hat{P}$

We use Nyquist stability arguments to analyze stability of $\hat{P}$. Recall that $\hat{P}$ is the closed-loop transfer function of the TCP/AQM network without DiffServ as described in (8). The open-loop transfer function of

$$\hat{P}(s) \triangleq \frac{L(s)}{1+L(s)}$$

is given by

$$L(s) \triangleq -\frac{1}{s-\frac{\partial f}{\partial q}} \frac{k_{aqm}(\frac{s}{z_{aqm}}+1)}{s} \sum_{i=1}^{n} e^{-s\tau_i} \frac{\partial g_i}{\partial p} \frac{1}{s-\frac{\partial g_i}{\partial W_i}} \frac{\eta_i}{\tau_i}. \tag{24}$$

Since $L(s)$ has a pole at the origin, it is necessary that the Nyquist contour Γ includes an infinitesimal semicircle Γ_ϵ around $s = 0$ described by (see Figure 7(a)).As s traverses from $-j\epsilon$ to $+j\epsilon$ along Γ_ϵ, θ changes from -90° to $+90^\circ$ counterclockwise. The corresponding Nyquist plot of $L(s)$ can be determined by evaluating (9) along (10). In the limit we have

$$\lim_{\epsilon \to 0} L(\epsilon e^{j\theta}) = \frac{1}{-\frac{\partial f}{\partial q}} \frac{k_{aqm}}{\epsilon e^{j\theta}} \sum_{i=1}^{n} -\frac{\partial g_i}{\partial p} \frac{\eta_i}{\tau_i} \frac{1}{-\frac{\partial g_i}{\partial W_i}}$$

The contour indentation near origin Γ_ϵ is mapped by $L(s)$ into a semi-infinite circle covering the RHP of the complex plane. The generic Nyquist plot in Figure 7(b), which preserves its form no matter the magnitude of $k_{aqm} > 0$, is similar to that of our $L(s)$. Any instabilities in $\hat{P}(s)$ will be the result of encirclements by the Nyquist plot of $L(s)$ over the range $\omega \in (\epsilon, +\infty) \cup (-\epsilon, -\infty)$. Define $L(j\omega) = k_{aqm}\tilde{L}(j\omega)$. The plot of $\tilde{L}(j\omega)$ crosses the negative real-axis at frequencies in the set $\Omega = \{\omega : \angle\tilde{L}(j\omega) = -180^\circ\}$. Let ω_4 be the frequency such that $|\tilde{L}(j\omega_4)| = \max_{\omega\in\Omega} |\tilde{L}(j\omega)|$. If $k_{aqm} < \frac{1}{|\tilde{L}(j\omega_4)|}$ then $|L(j\omega)| < 1$ implying stability of $\hat{P}$. To conclude,

$$k_{aqm} < \frac{1}{|\tilde{L}(j\omega_4)|} \Longrightarrow \hat{P} \text{ stable.} \tag{25}$$

REFERENCES

[1] V. Jacobson, K. Nichols, and K. Poduri, "An expedited forwarding PHB," *RFC2598*, 1999.

[2] J. Heinanen, F. Baker, W. Weiss, and J. Wroclawski, "Assured forwarding goup," *RFC2597*, 1999.

[3] K.K. Ramakrishnan, and S. Floyd, "Proposal To Add Explicit Congestion Notification (ECN) to IP," *RFC 2481*, 1999.

[4] S. Sahu, P. Nain, D. Towsley, C. Diot, and V. Firoiu, "On Achievable Service Differentiation with Token Bucket Marking for TCP," *Procs. ACM SIGMETRICS*, pg. 23-33, 2000.

[5] I. Yeom, and A. L. N. Reddy, "Modeling TCP behavior in a Differentiated-Services Network," *ACM/IEEE Trans. Networking*, 2001.

[6] M. Goyal, A. Durresi, P. Misra, C. Liu, R. Jain, "Effect of Number of Drop Precedences in Assured Forwarding," *Procs. GlobeCom*, 1999.

[7] Y. Chait, C.V. Hollot, V. Misra, D. Towsley, H. Zhang,and C.S. Lui, "Throughput Guarantees for TCP Flows Using Adaptive Two Color Marking and Multi-Level AQM," *Procs. INFOCOM*, pg. 837-844, 2002.

[8] C. V. Hollot, V. Misra, D. Towsley, and W. B. Gong, "On designing improved controllers for aqm routers supporting tcp flows," in *Procs. INFOCOM*, 2001.

[9] Y. Chait, C.V. Hollot, V. Misra, D. Towsley, H. Zhang, C.S. Lui, and Y. Cui "Guaranteed Throughput Using Adaptive Two-Level Coloring at the Network Edge and Preferential Dropping at the Core," *ACM/IEEE Trans. Networking*, submitted; available upon request.

[10] V. Misra, W. Gong, and D. Towsley. "Fluid-based analysis of a network of AQM routers supporting TCP flows with an application to RED," *Procs. ACM SIGCOMM*, 2000.

[11] S. H. Low, F. Paganini, and J. C. Doyle, "Internet Congestion Control," *IEEE Control Systems Magazine*, 22(1), pg. 28-43, 2002.

[12] S. Blake, D. Black, M. Carlson, E. Davies, Z. Wang, and W. Weiss, "An architecture for Differentiated Services," *RFC2475*, Network Working Group, Dec. 1998; also in *Proc. SIGCOMM'00*, 2000.

[13] D. D. Clark, and W. Fang, "Explicit allocation of best effort packet delivery service." *IEEE/ACM Transactions on Networking*, 1998.

[14] Y. Chait, and C.V. Hollot,"Fixed Point of a TCP/RENO DiffServ Network with a Single Congested Link ," DACS Lab, *Technical Report DACS02-07*, 2003.

[15] K. Ogata, *Modern Control Engineering*, 4th Edition, Prentice Hall, NJ. 2002.